Perturbation of the PET Process in "Fluorophore–Spacer-–Receptor" Systems Through Structural Modification: Transition Metal Induced Fluorescence Enhancement and Selectivity

Bamaprasad Bag and Parimal K. Bharadwaj*
Chemistry Department, Indian Institute of Technology Kanpur, 208016 India
Email: pkb@iitk.ac.in

Supporting Information

Captions for the figures and Tables:

Table ST1: Crystallographic Data and Structure Refinement for **2**, **3**, **4**, **5**, **7** and **8**.

	2	**3**	**4**	**5**	**7**	**8**
Empirical Formula	$C_{25}H_{24}N_4O_4$	$C_{25}H_{25}N_3O_2$	$C_{24}H_{24}N_4O_2$	$C_{10}H_{14}N_4O_4$	$C_{23}H_{20}N_4O_4$	$C_{29}H_{22}N_6O_8$. $(CH_3)_2$ S O
Formula weight	444.48	399.48	400.47	254.25	416.43	660.65
Temperature (K)	293	293	293	293	293	293
Radiation	Mo Kα	Mo Kα	Mo Kα	Mo Kα	Mo Kα	Mo Kα
Wavelength (Å)	0.71073	0.71073	0.71073	0.71073	0.71073	0.71073
Crystal system	Triclinic	Monoclinic	Monoclinic	Triclinic	Monoclinic	Triclinic
Space group	P –1	P 2_1/c	P 2_1/c	P –1	P 2_1	P –1
a, Å	9.859(5)	9.395(2)	12.453(2)	5.486(2)	7.9210(8)	10.956(5)
b, Å	10.831(5)	21.403(2)	6.328(4)	10.556(2)	14.295(14)	12.656(6)
c, Å	11.314(5)	10.120(5)	26.349(2)	10.630(2)	8.7995(9)	12.773(2)
α (°)	88.63(5)			83.38(4)		112.54(2)
β (°)	69.45(5)	98.79(6)	93.88(5)	75.65(6)	91.71(2)	103.22(2)
γ(°)	75.31(5)			79.62(3)		101.28(6)
V, Å^3	1091.5(9)	2011.0(11)	2071.6(2)	585.0(3)	995.91(17)	1511.3(10)
Z	2	4	4	2	2	2
ρ_{calc} Mg/m^3	1.352	1.319	1.284	1.443	1.389	1.452
μ, mm^{-1}	0.094	0.085	0.084	0.114	0.097	0.174
F (000)	468	848	848	268	436	688
T (min.)	0.9797	0.9849	0.9810	0.9776	0.9827	0.9594
T (max.)	0.9843	0.9890	0.9851	0.9821	0.9874	0.9660
Refl. (collected)	2841	4997	2702	1541	4277	3934
Refl. (Unique)	1943	3582	1413	1113	3748	2877
GOOF on F^2	1.056	0.847	0.979	1.027	0.987	1.071
R_{Final} R1 =	0.0401	0.0566	0.0492	0.0852	0.0524	0.0483
$I > 2\sigma(I)$ *w*R2 =	0.1074	0.1379	0.1150	0.2209	0.1269	0.1477
R_{all} R1 =	0.0745	0.0857	0.1557	0.1179	0.0595	0.0843
(all data) *w*R2 =	0.1259	0.1585	0.1539	0.2429	0.1322	0.1677

Crystal data for **5.H**: C_{10} H_{15} N_4 O_8 Cl; M = 354.71; pale yellow blocks, orthorhombic, space group $Pca2_1$, *a* = 13.687(2) Å, *b* = 6.130(3) Å, *c* = 17.228(3) Å, U = 1445.5(6) Å^3, T = 293 K, Z = 4, μ(Mo K_α) = 0.316 mm^{-1}, F(000) = 736, 3541 reflection data with 212 parameters, 3450 [$I \geq 2\ \sigma(I)$] unique reflections were used in all calculations. The final R1 = 0.0296, WR2 = 0.0800, S = 0.953.

Refinement methods: Full-matrix least squares on F^2.
$R = \Sigma\,|\,|Fo| - |Fc|\,| / |Fo|$; *w*R2 = $[\Sigma[w(F_o^2 - F_c^2)^2] / \Sigma[w(F_o^2)^2]]^{1/2}$; $w = 1/\sigma(F)$.

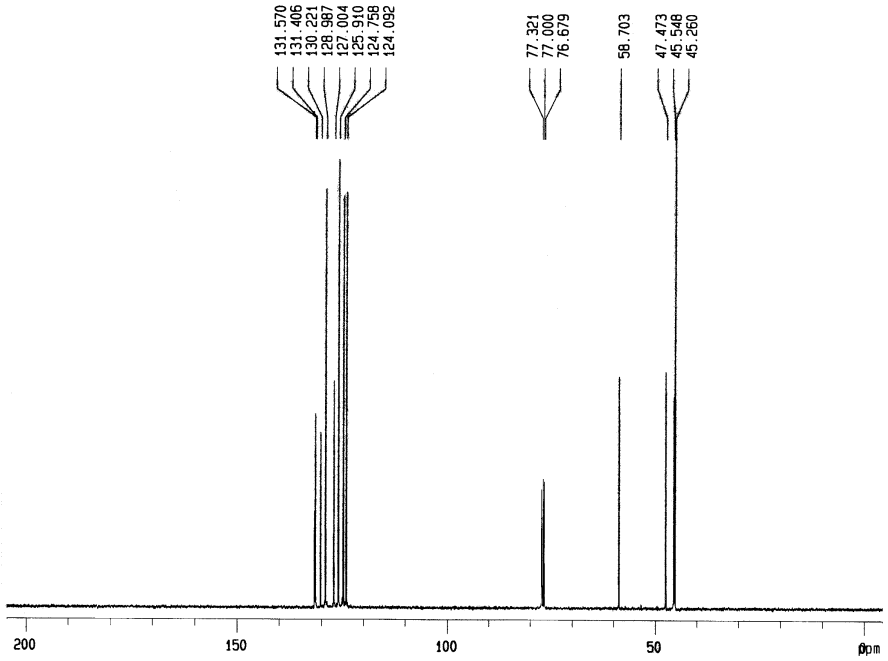

Figure S1: 100 MHz ^{13}C-NMR spectrum of **1**.

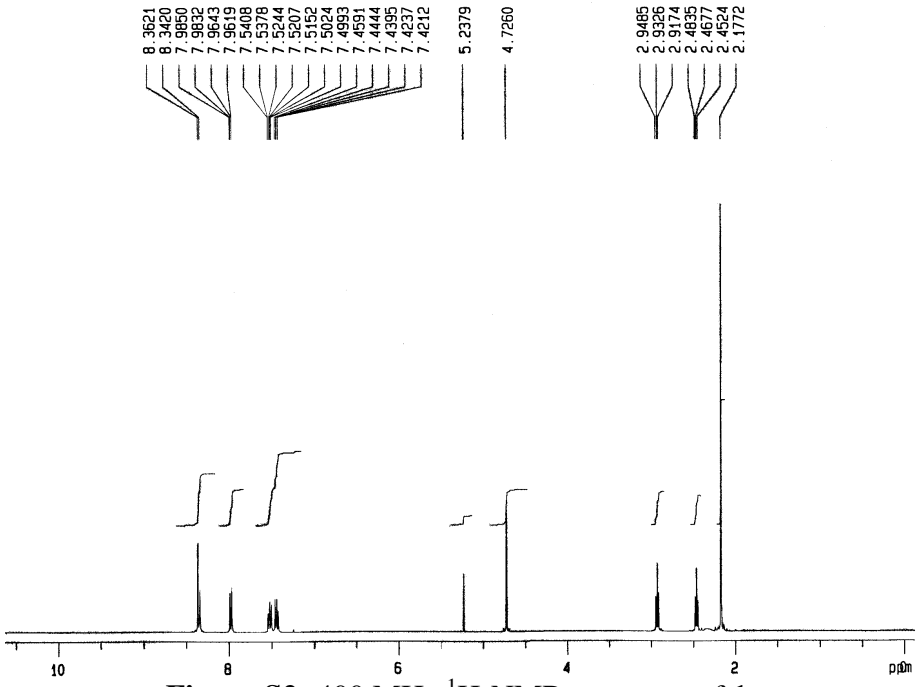

Figure S2: 400 MHz ^{1}H-NMR spectrum of **1**.

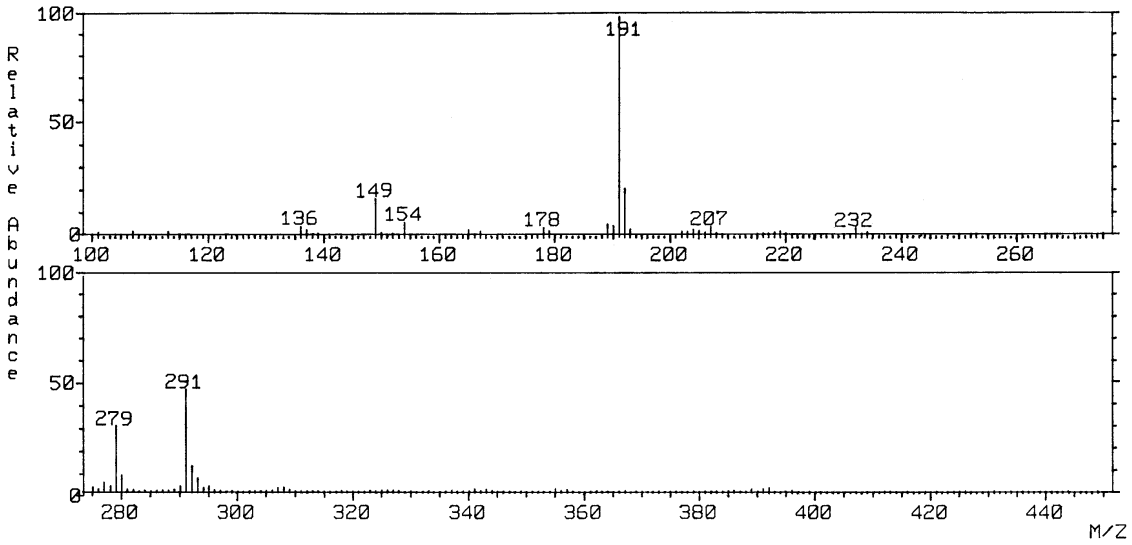

Figure S3: FAB-MASS spectrum of **1 [279, (M + 1)$^{+}$]**.

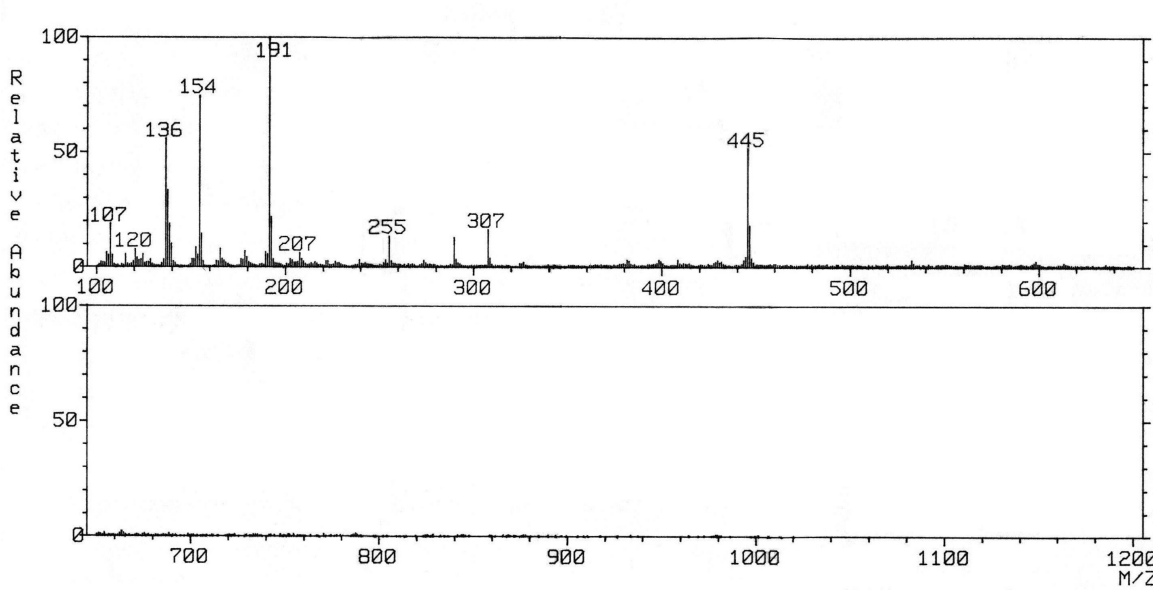

Figure S4: FAB MASS spectrum of **2**.

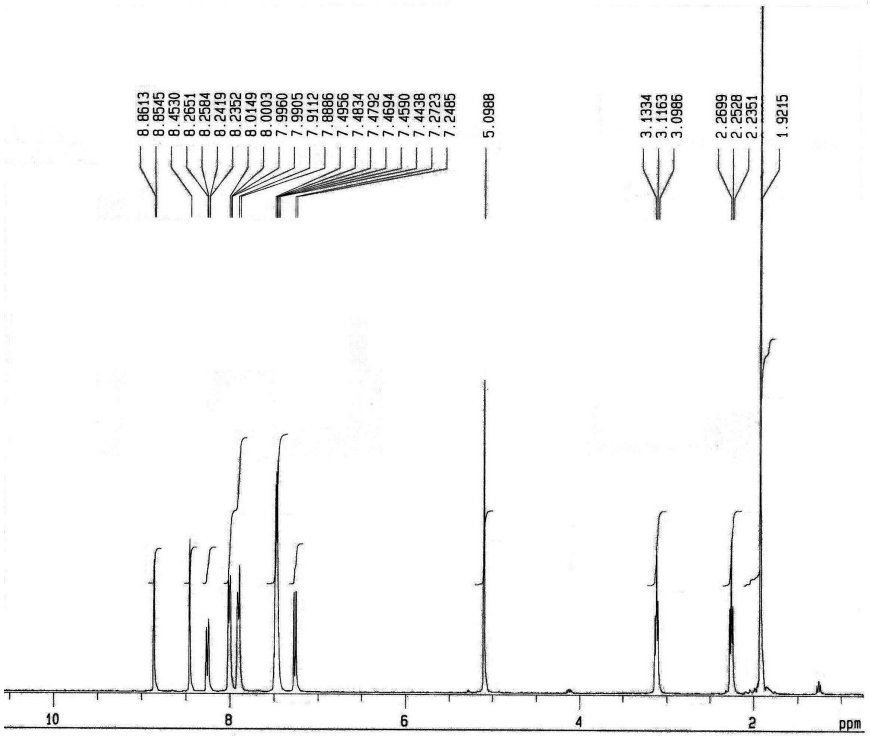

Figure S5: 400 MHz ^{1}H-NMR spectrum of **2**.

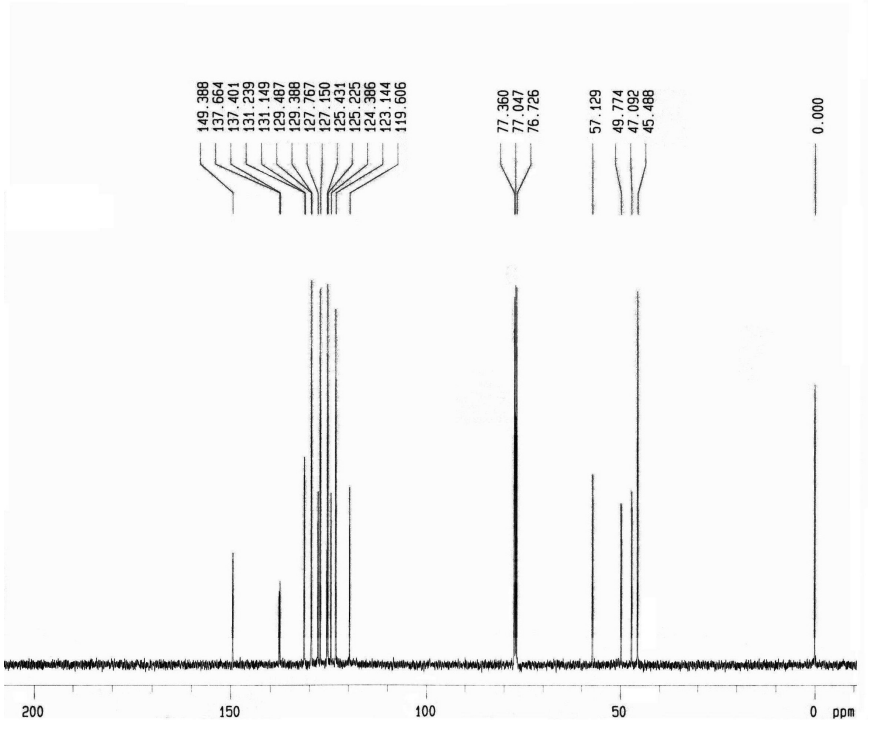

Figure S6: 100 MHz ^{13}C-NMR spectrum of **2**.

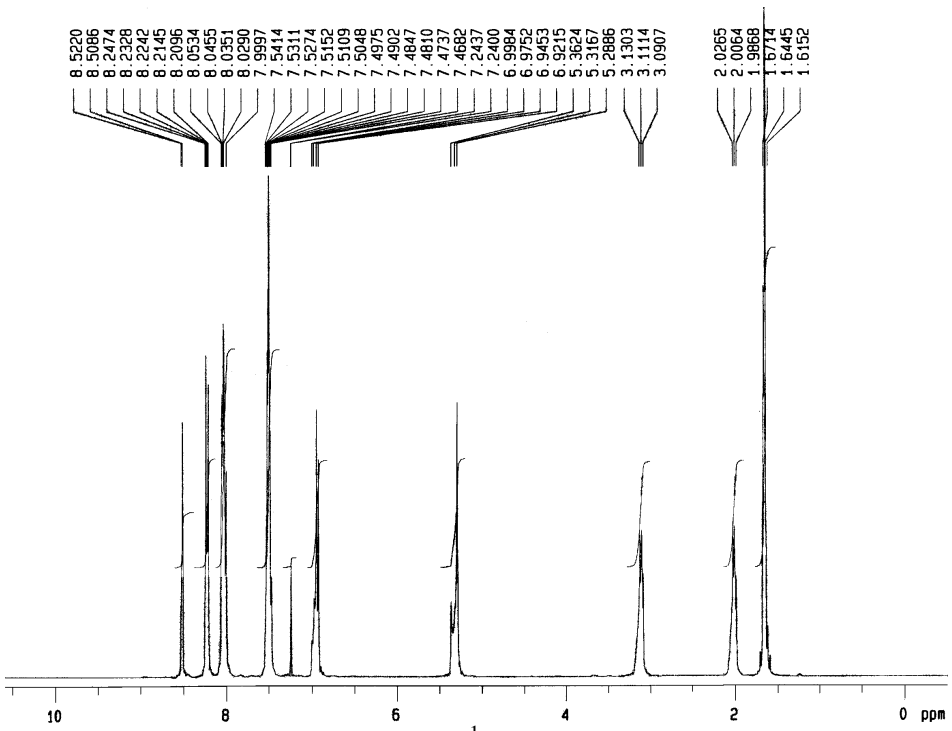

Figure S7: 400 MHz ^{1}H-NMR spectrum of **3**.

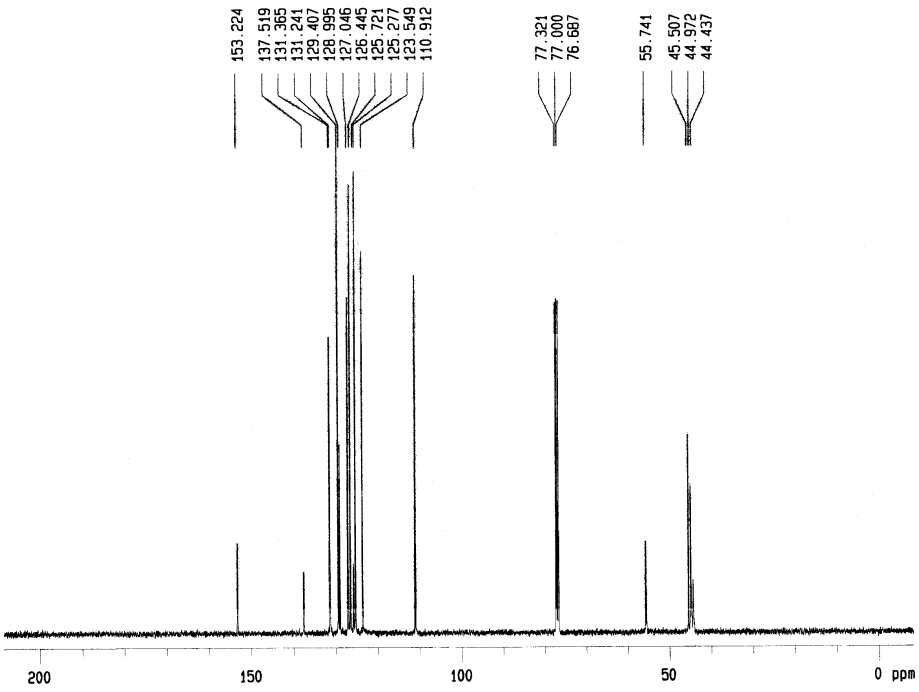

Figure S8: 100 MHz ^{13}C-NMR spectrum of **3**.

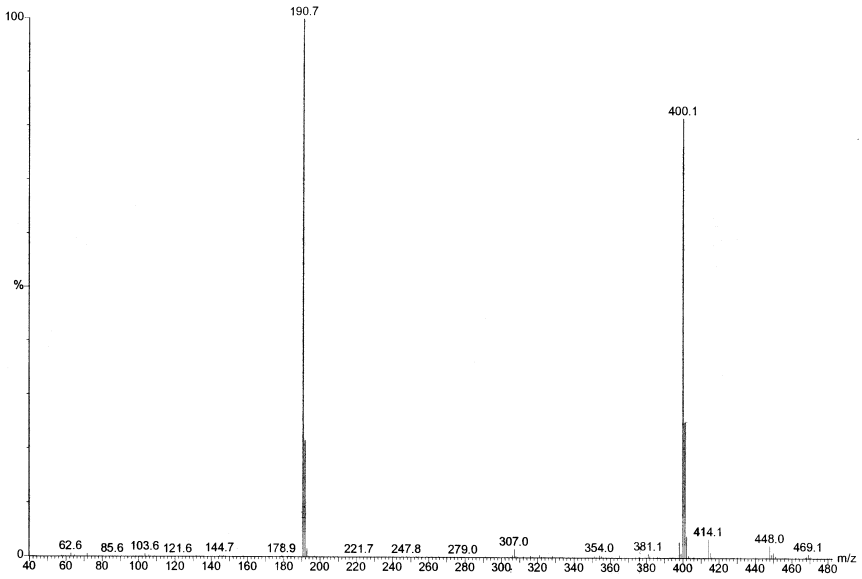

Figure S9: ESI-MS spectrum of **3**.

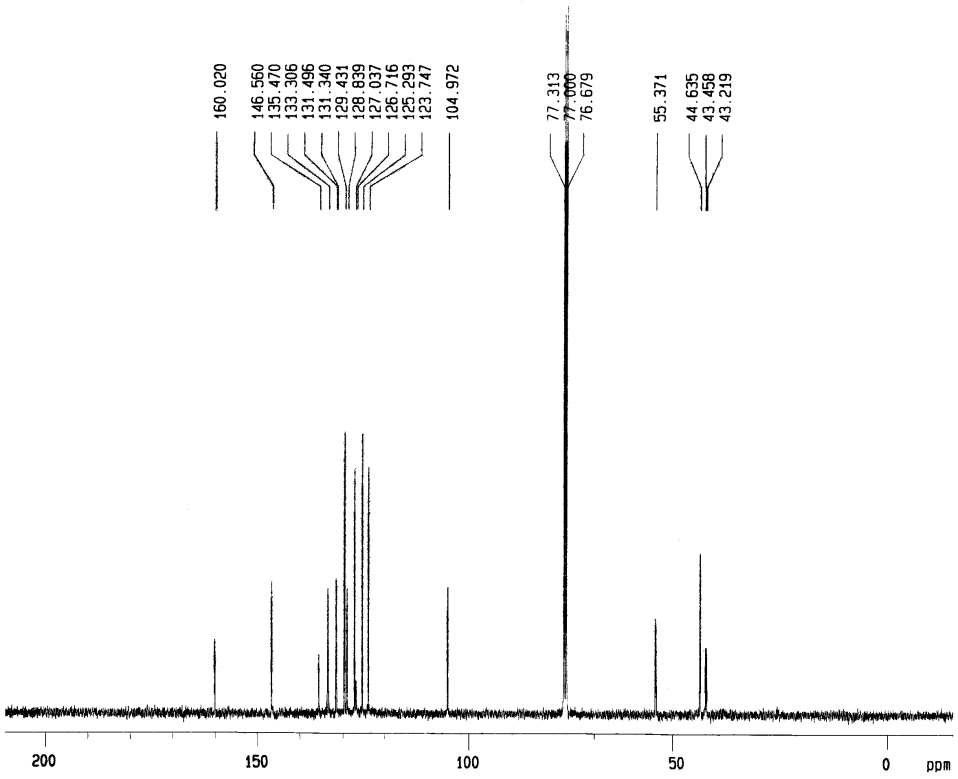

Figure S10: 100 MHz ^{13}C-NMR spectrum of **4**.

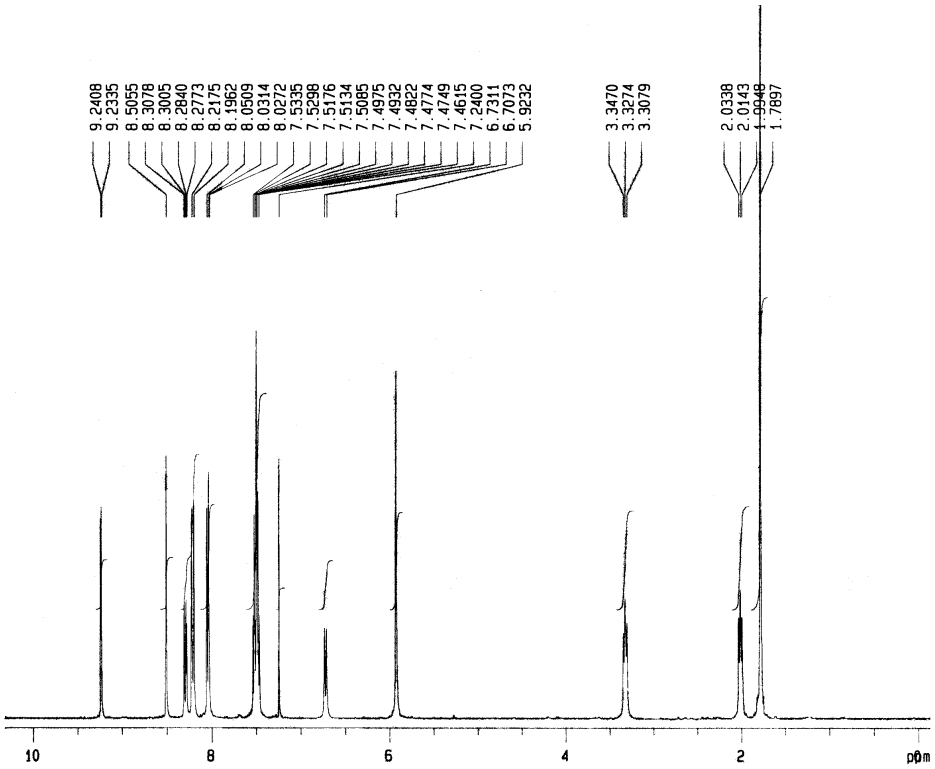

Figure S11: 400 MHz ^{1}H-NMR spectrum of **4**.

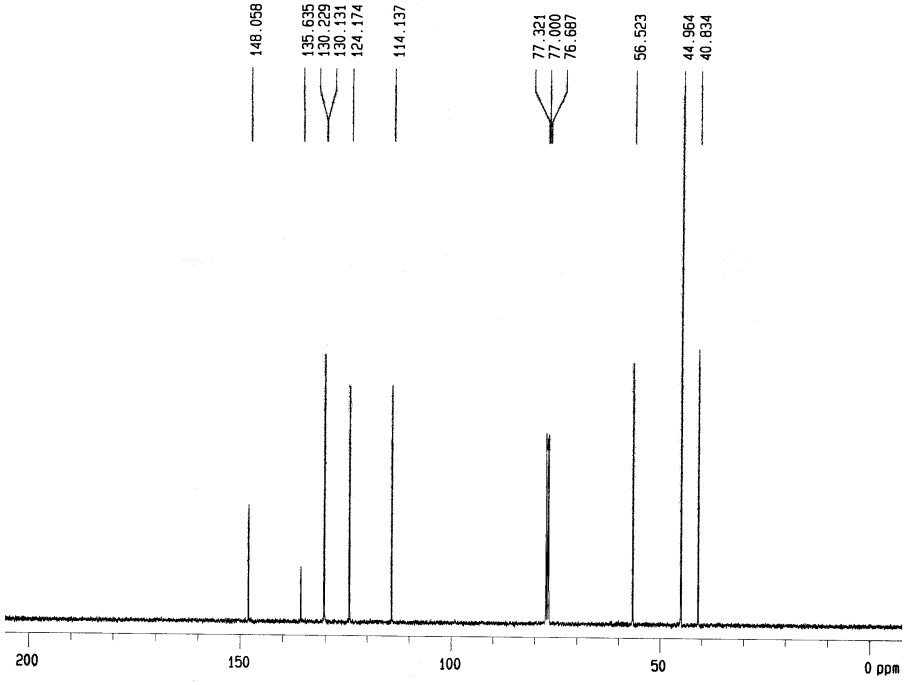

Figure S12: 100 MHz ^{13}C-NMR spectrum of **5**.

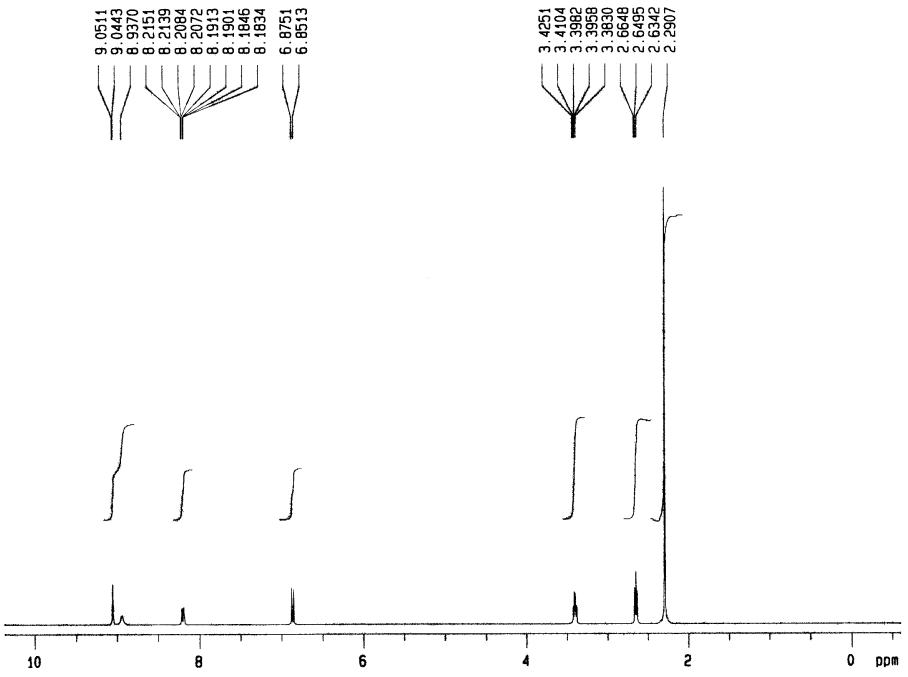

Figure S13: 400 MHz ^{1}H-NMR spectrum of **5**.

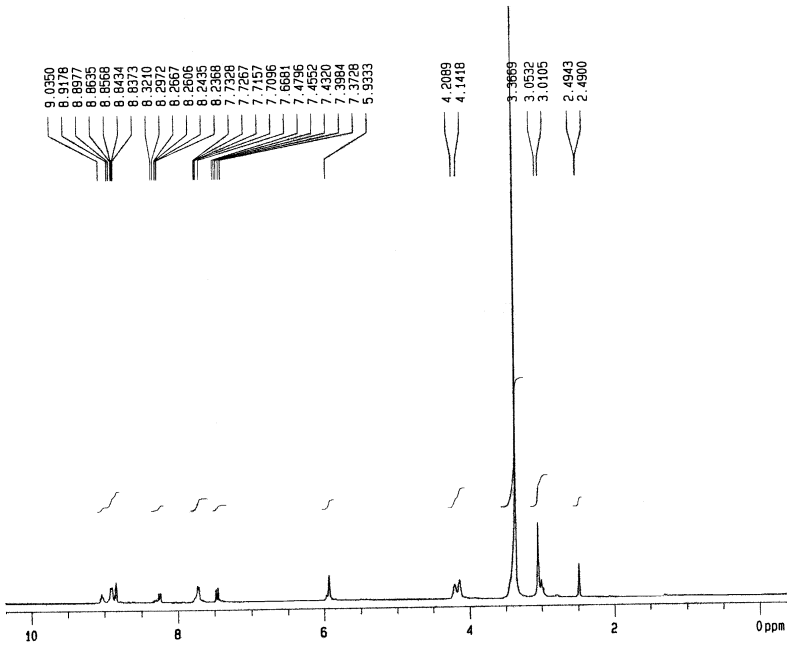

Figure S14: 400 MHz ^{1}H-NMR spectrum of **6**.

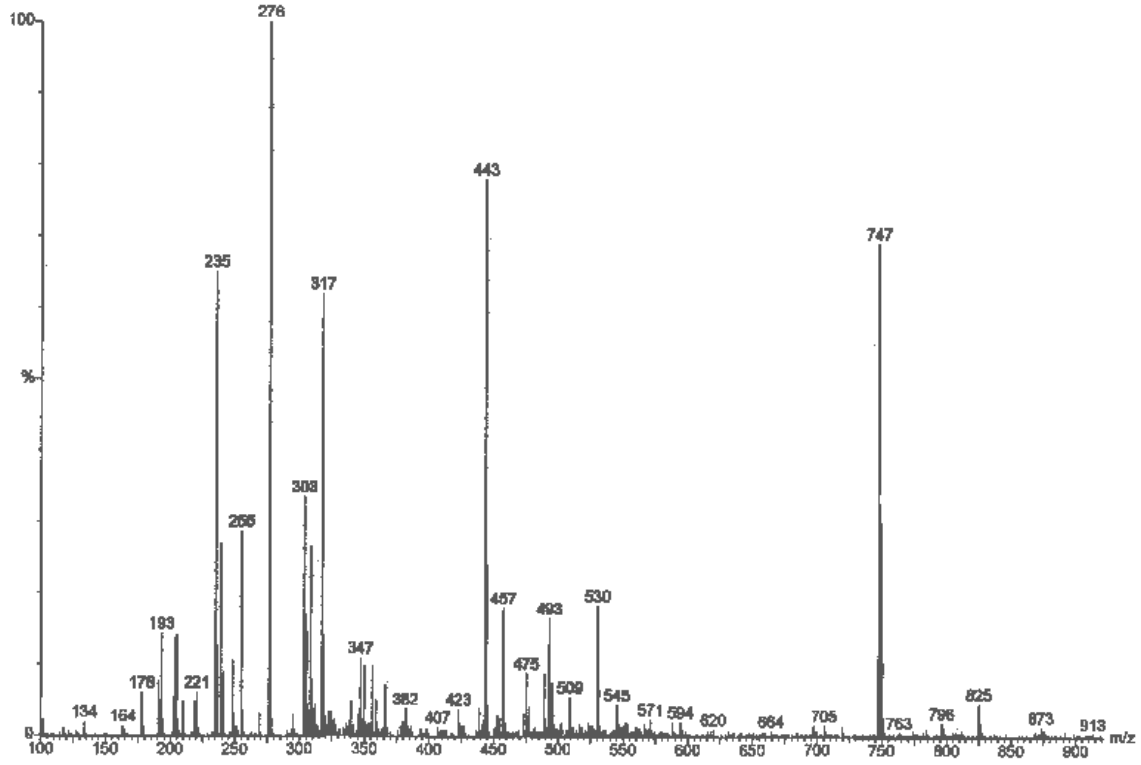

Figure S15: ESI-MS spectrum of **6**.

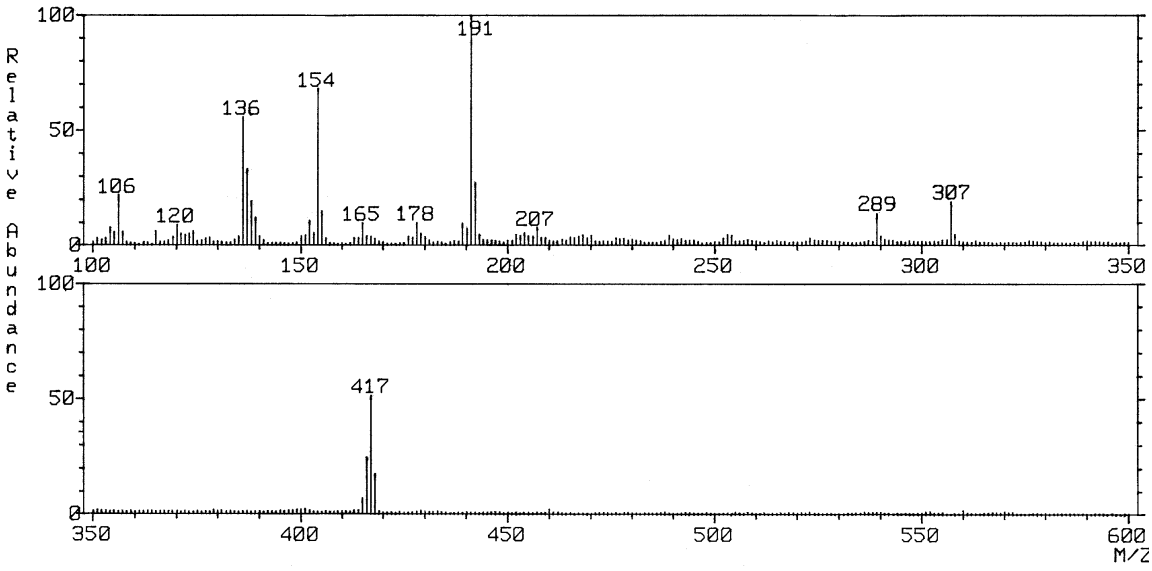

Figure S16: FAB-MASS spectrum of **7**.

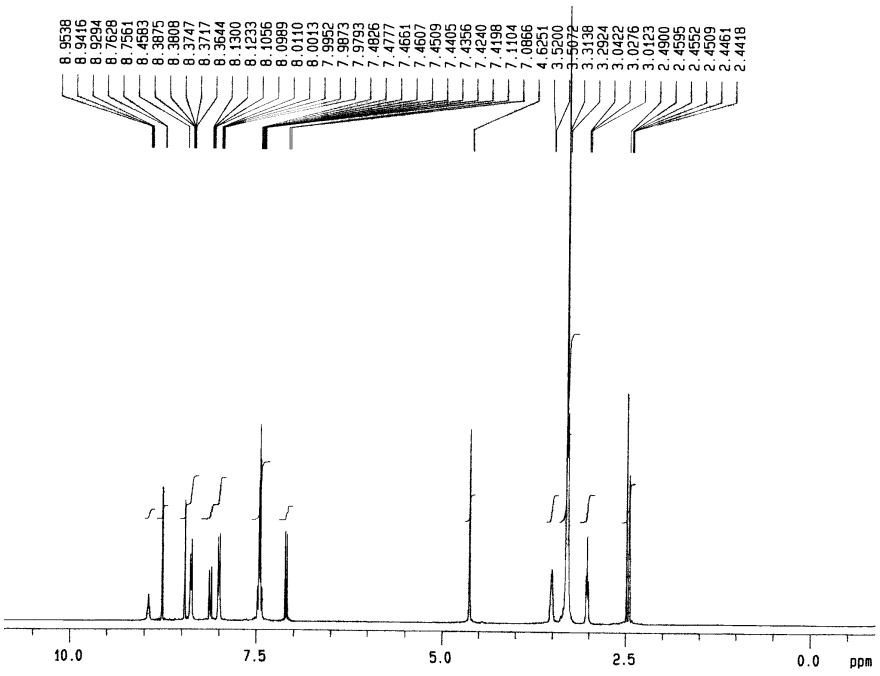

Figure S17: 400 MHz ^{1}H-NMR spectrum of **7**.

Absorption Spectroscopy:

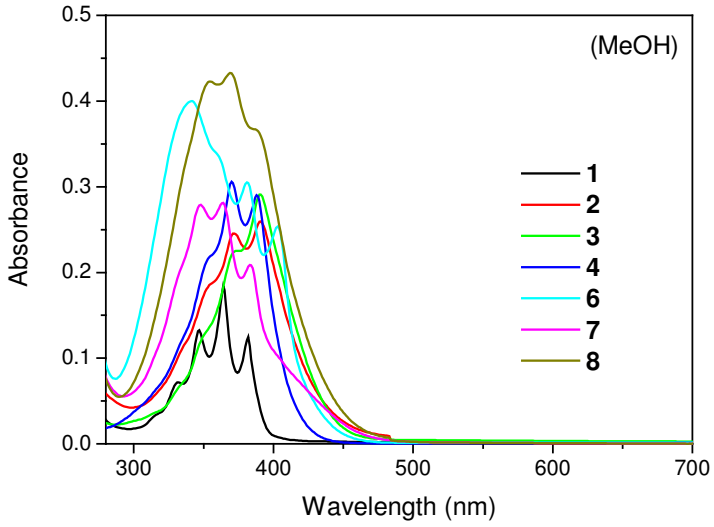

Figure S18: Absorption spectra of the fluorophoric systems (**1**-**8**) in MeOH at ~1× 10^{-5} M concentration.

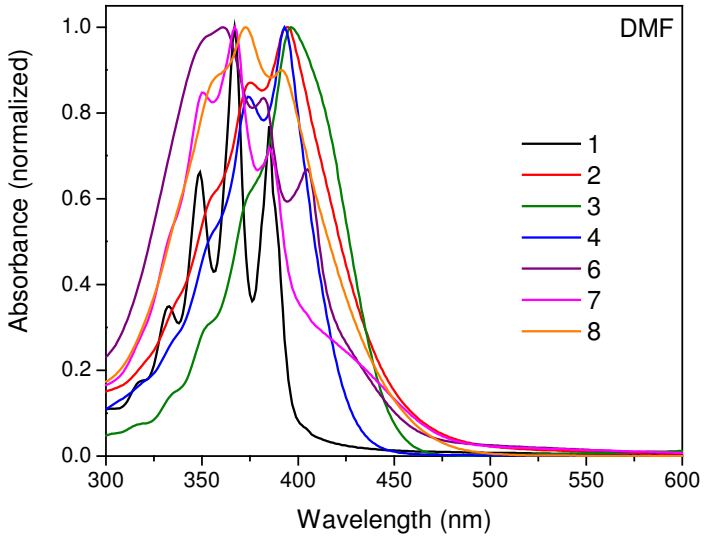

Figure S19: Absorption spectra (normalized) of the fluorophoric systems in DMF at ~1 × 10^{-5} M concentration. The vibrational transitions get modulated as a function of electronic withdrawing substituents.

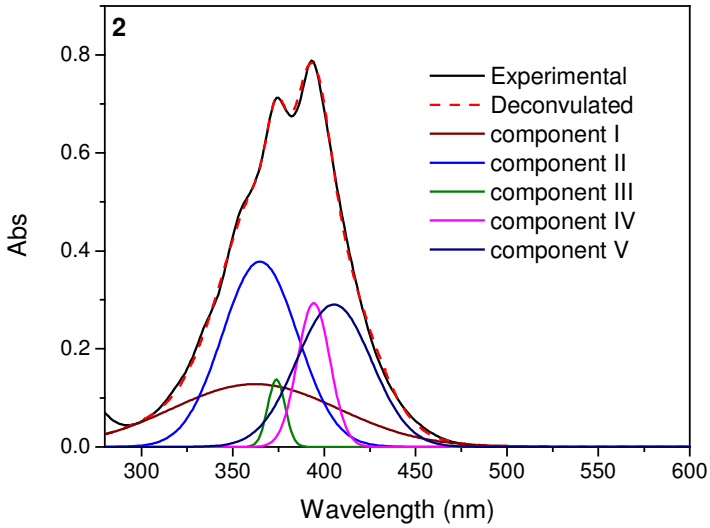

Figure S20: Curve fitted component distribution diagram of the absorption spectra of **2** in dry THF at ~ 3 × 10^{-5} M concentration showing the presence of both the components of anthracene π–π* and the ICT transitions of 2,4-dinitrobenzene group.

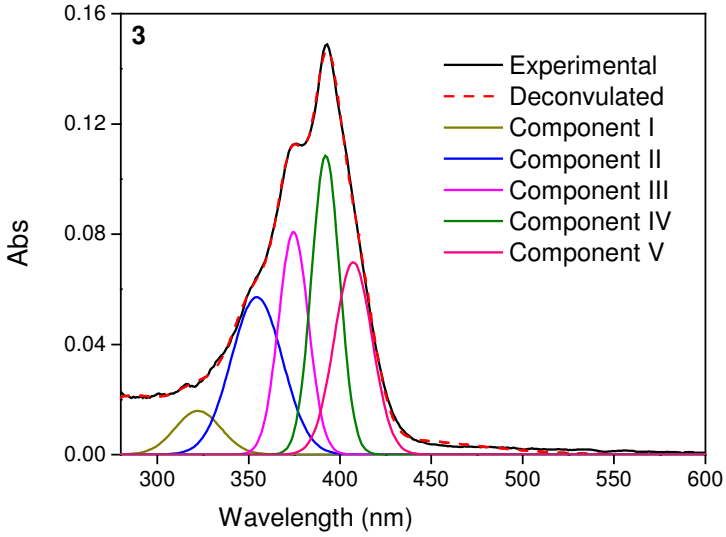

(a)

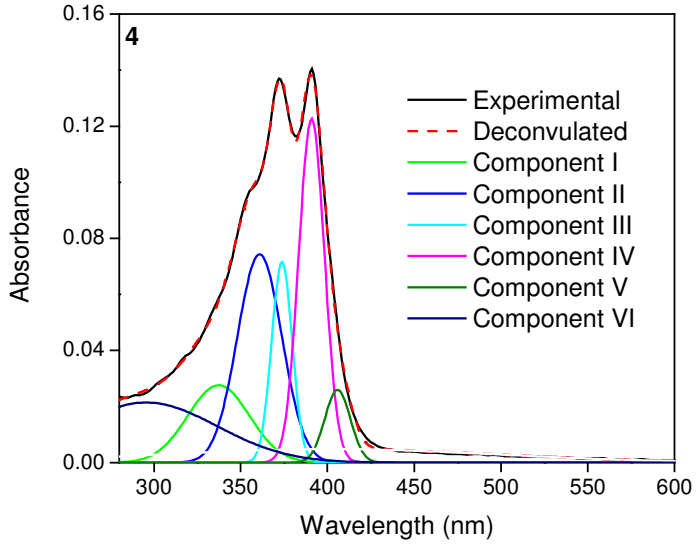

(b)

Figure S21: Curve fitted to the absorption spectra of **3** (a) and **4** (b) in dry THF at ~0.5 $\times 10^{-5}$M concentration shows the presence of all the components of anthracene π–π^* and the nitrobenzene/nitropyridine ICT transitions.

Table ST2: Absorption of the fluorophoric systems(**1-8**) in various solvents:

System (s)	Solvents	Absorption λ, nm (ε, dm^3 mol^{-1} cm^{-1})
1	Cyclohexane	381(8706) 368(9249) 353(6095) 334(2801)
	$CHCl_3$	384(10698) 367(17070) 350(12329) 334(6606)
	THF	385(9047) 366(9767) 348(6124) 331(2962) 259(8315)
	MeOH	382(12233) 364(18228) 347(13015) 332(6942) 257(16520)
	Acetone	382(11751) 365(18072) 347(12456) 331(6759)
	EtOH	382(12126) 366(17212) 347(12270) 332(6587)
	MeCN	384(9630) 365(10136) 347(6523) 331(3243)
	DMF	385(12024) 363(19019) 347(13117) 331(7059)
2	Cyclohexane	392(18674) 372(19108) 356(12999)
	DCM	394(21815) 375(20150) 355(17439)
	$CHCl_3$	393(30391) 373(23674) 355(19156)
	THF	393(25489) 373(23550) 355(17385) 274(6398)
	MeOH	391(19156) 372(18053) 353(16644)
	Acetone	392(23352) 373(20869) 353(17583)
	EtOH	394(25671) 372(23789) 353(17541)
	MeCN	392(25358) 373(22370) 352(16947)
	DMSO	397(26674) 377(23894) 350(17992)
3	Cyclohexane	390(23856) 371(19506) 256(29876)
	$CHCl_3$	395(31546) 375(22894) 256(32534)
	THF	393(32085) 377(26172) 262(14110)
	MeOH	391(28595) 372(21907) 350(12068)
	Acetone	393(32862) 373(23230) 350(s)
	EtOH	391(28008) 373(22572) 255(29677)
	MeCN	394(31293) 373(21872) 351(11145) 250(31187)
	DMF	398(32682) 372(23935) 351(14809)
4	Cyclohexane	389(22176) 370(20684) 353(15778)
	$CHCl_3$	393(30554) 374(27887) 355(18221) 256(45366)
	THF	392(29333) 371(30385) 354(28327) 261(15958)
	MeOH	388(28902) 370(30461) 353(21464)
	Acetone	390(33515) 372(31402) 354(20670)
	EtOH	389(31796) 371(33754) 355(24462) 253(57346)
	MeCN	390(28740) 372(26495) 352(16597) 251(32351)
	DMF	391(28254) 372(25875) 352(17698)
6	Cyclohexane	381(n. d.) 340(n. d.) 262(n. d.)
	$CHCl_3$	383(n. d.) 342(n. d.) 260(n. d.)
	THF	393(23516) 351(39594) 259(147172)
	MeOH	403(25315) 381(30595) 360(33868) 341(40214) 258(16648)
	Acetone	400(25780) 377(32860) 352(41630)

	EtOH	404(24211) 381(29378) 341(38833) 259(164433)
	MeCN	402(27247) 379(33979) 347(43890) 258(177635)
	DMF	407(27543) 377(35635) 340(40559)
7	Cyclohexane	386(15212) 368(19774) 352(20177)
	$CHCl_3$	420(s) 386(14838) 366(21927) 350(23319) 256(47394)
	THF	384(18338) 365(29427) 349(30229) 260(28231)
	MeOH	383(20986) 364(29568) 348(29315) 258(16648)
	Acetone	383(17186) 364(25616) 349(24084)
	EtOH	384(23915) 364(31715) 348(31615) 253(179538)
	MeCN	383(15607) 364(28787) 349(24256) 256(22629)
	DMF	381(22720) 363(30177) 347(28886)
8	Cyclohexane	394(n. d.) 375(n. d.) 355(n. d.)
	$CHCl_3$	393(34491) 373(41311) 355(43148) 257(158531)
	THF	393(31098) 372(36411) 356(35536) 256(22367)
	MeOH	389(35056) 369(41824) 355(40784) 253(166176)
	Acetone	391(29593) 371(34433) 356(32527)
	EtOH	387(33858) 368(39960) 353(39852) 254(169596)
	MeCN	389(39168) 371(45008) 353(41648) 253(171744)
	DMF	386(40440) 267(44675) 351(43738)

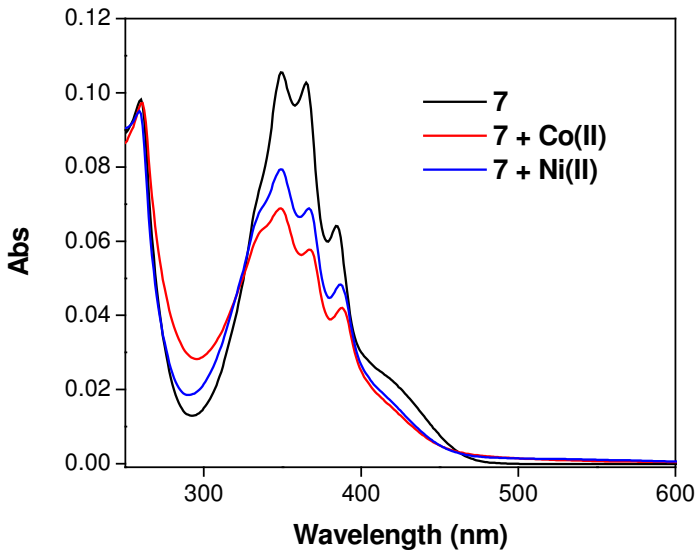

Figure S22: Absorption spectra of **7** alone and in presence of Co(II) and Ni(II) in dry THF at ~ 0.5 $\times 10^{-5}$ M concentration.

Table ST3: Absorption and molar extinction coefficients of fluorophoric systems in dry THF in presence of various ionic inputs.

Fluorophoric systems	Ionic input	λ, nm (ε, $dm^3\ mol^{-1}\ cm^{-1}$)
1	-	385(9047) 366(9767) 348(6124) 331(2962) 319(1302) 259(8315)
	Mn(II)	386(4923) 367(6036) 349(4316) 332(2715) 260(8569)
	Fe(II)	386(8123) 367(9425) 348(6159) 333(3262) 260(9992)
	Co(II)	387(6987) 368(8328) 349(6249) 334(3920) 262(11228)
	Ni(II)	387(7502) 368(8785) 349(5563) 333(2761) 261(10840)
	Cu(II)	388(7095) 368(8549) 350(5849) 334(3376) 262(10918)
	Zn(II)	387(7866) 367(9561) 349(6220) 333(3071) 260(7909)
	H^+	389(6674) 369(8425) 351(5918) 336(3097) 261(7269)
2	-	394(25489) 373(23550) 355(17385) 274(6398)
	Mn(II)	393(21638) 373(23399) 355(20177) 274(9971)
	Fe(II)	393(22174) 374(20332) 355(14532) 274(8044)
	Co(II)	393(17914) 373(19237) 355(17629) 274(9075)
	Ni(II)	393(16275) 373(18201) 356(16743) 276(12324)
	Cu(II)	392(19560) 373(20468) 355(17714) 274(11369)
	Zn(II)	393(15728) 373(17213) 355(15616) 271(12438)
	NH_4^+	393(23395) 375(21625) 355(15811) 274(7951)
3	-	393(32085) 377(26172) 262(14110)
	Mn(II)	391(26456) 370(28723) 264(18785)
	Fe(II)	391(28116) 370(29014) 263(18619)
	Co(II)	391(21451) 371(28101) 262(17062)
	Ni(II)	391(26658) 371(28720) 263(15494)
	Cu(II)	391(25996) 371(28627) 263(15423)
	Zn(II)	391(26356) 371(28582) 263(14488)
	H^+	389(27534) 369(29886) 262(18031)
4	-	392(29333) 371(30385) 354(28327) 261(12982)
	Mn(II)	390(27008) 371(23983) 354(21740) 259(18662)
	Fe(II)	390(22720) 370(30285) 355(27022) 261(15958)
	Co(II)	390(16098) 370(23397) 354(20417) 262(16485)
	Ni(II)	388(20151) 369(30147) 354(27874) 260(14782)
	Cu(II)	388(19585) 369(29710) 354(27651) 261(15951)
	Zn(II)	390(19845) 369(30177) 354(27522) 261(14619)
	H^+	390(20793) 368(31478) 354(29143) 261(17975)
5	-	352(19778) 264(8336) 232(9525)
	Mn(II)	342(18516) 265(15370) 233(14529)
	Fe(II)	343(18017) 265(14473) 233(14116)
	Co(II)	340(16669) 266(12911) 232(13634)

	Ni(II)	342(17684)	265(9353)	230(10585)	
	Cu(II)	340(17585)	265(12686)	234(13760)	
	Zn(II)	340(16669)	266(12911)	232(13634)	
	H^+	343(18162)	265(9308)	231(8839)	
6	-	393(23516)	351(39594)	259(147172)	
	Mn(II)	393(21719)	341(36141)	251(143563)	
	Fe(II)	393(22984)	348(38875)	251(146251)	
	Co(II)	393(24625)	343(37781)	251(149278)	
	Ni(II)	393(23405)	341(37953)	251(146750)	
	Cu(II)	393(22594)	346(39200)	251(148994)	
	Zn(II)	393(23203)	339(38578)	251(152125)	
	H^+	393(23673)	339(39440)	251(147389)	
7	-	384(18338)	365(29427)	349(30229)	260(28138)
	Mn(II)	388(13209)	368(18625)	349(22550)	259(26074)
	Fe(II)	385(14585)	365(22636)	349(24871)	260(27421)
	Co(II)	388(12579)	368(16504)	349(19742)	261(27851)
	Ni(II)	387(13840)	368(19570)	349(22751)	259(27220)
	Cu(II)	388(12579)	368(17708)	349(22092)	259(27536)
	Zn(II)	388(13209)	368(18711)	349(22951)	259(26275)
	Cd(II)	385(14928)	365(23181)	349(24842)	259(26074)
	H^+	386(19484)	365(35845)	353(36705)	260(33754)
8	-	393(31098)	372(36411)	356(35536)	256(22367)
	Mn(II)	392(26790)	367(33595)	359(33593)	258(33496)
	Fe(II)	383(23098)	363(34500)	348(31439)	256(31228)
	Co(II)	390(25527)	368(29964)	356(30472)	260(31325)
	Ni(II)	390(27536)	367(32621)	356(33042)	260(31066)
	Cu(II)	385(24781)	368(32492)	355(35166)	256(31358)
	Zn(II)	392(27632)	367(32686)	356(33107)	260(30840)
	Cd(II)	392(27730)	368(32847)	356(33236)	260(32429)
	H^+	392(23875)	368(30974)	356(39268)	257(34079)

Fluorescence Studies:

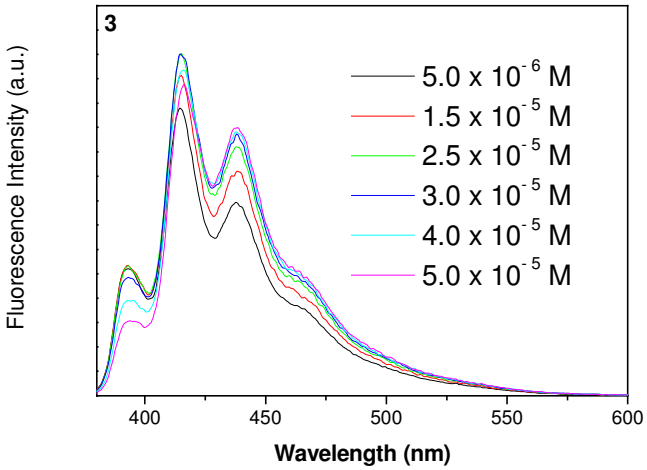

(a)

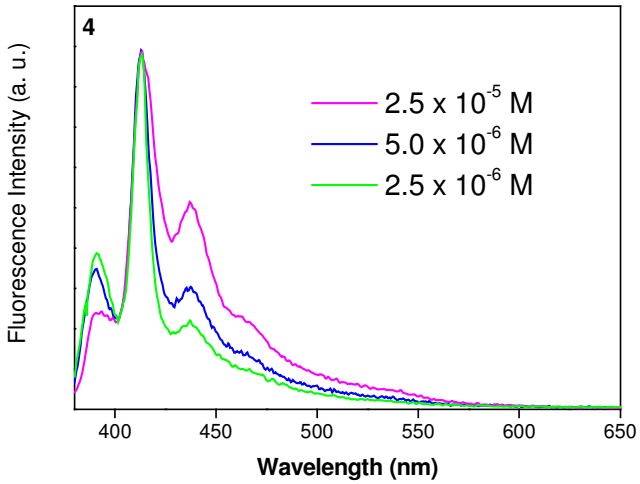

(b)

Figure S23: Fluorescence spectra of **3** (a) and **4** (b) in dry THF at different concentration.

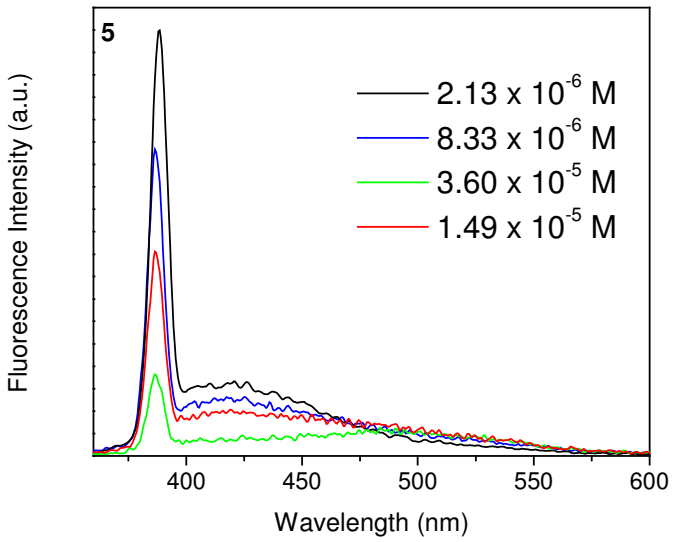

(a)

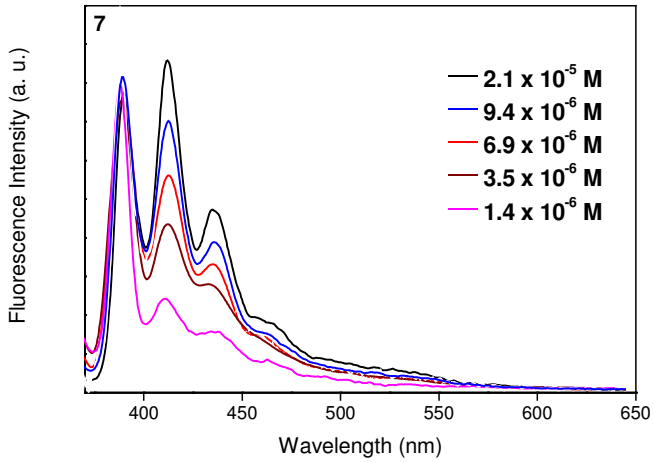

(b)

Figure S24: Fluorescence spectra of **5** (a) and **7** (b) in dry THF at different concentration.

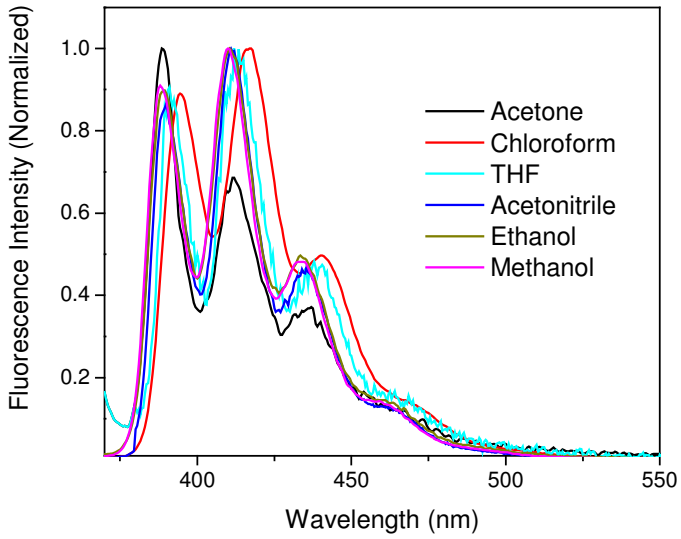

Figure S25: Normalized fluorescence spectra of **1** in various solvents.

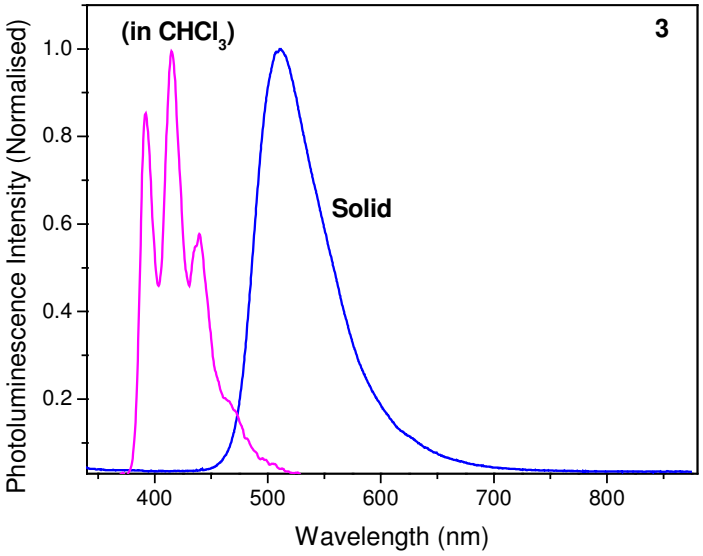

Figure S26: Normalized photoluminescence spectra of **3** in $CHCl_3$ solution as well as in solid state. The graph shows the emission to be well structured typical of anthracene in $CHCl_3$ solution centered at 416nm where as appears as a broad, structurless centered at 512 nm in solid state.

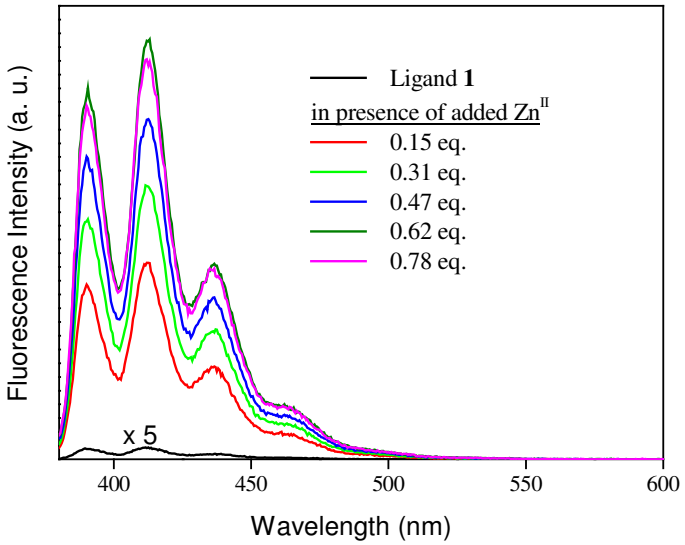

Figure S27: Fluorescence enhancement of **1** upon addition of Zn(II) in dry THF at 1.7 $\times 10^{-6}$ M concentration, λ_{ex} = 368 nm.

Table ST4: Fluorescence quantum yield and Fluorescence Enhancement of **2** upon addition of Cu (II) in dry THF at 5.0×10^{-6} M concentrations.

Cu (II) added (μM)	ϕ_F	Fluorescence Enhancement	Cu (II) added (μM)	ϕ_F	Fluorescence Enhancement
0.0	0.0004	1(standard)	30	0.0423	106
0.5	0.0056	14	40	0.0419	105
1.0	0.0071	18	50	0.0412	103
1.5	0.0173	43	60	0.0406	102
2.0	0.0269	67	70	0.0399	100
2.5	0.0305	76	90	0.0381	95
3.0	0.0328	82	100	0.0363	91
3.5	0.0355	89	150	0.0345	86
4.0	0.0388	97	200	0.0317	79
4.5	0.0409	102	300	0.0306	77
5.0	0.0421	105	400	0.0297	74
6.0	0.0430	108	500	0.0286	72
7.0	0.0431	108	600	0.0279	70
8.0	0.0431	108	700	0.0257	64
9.0	0.0429	108	800	0.0221	55
10	0.0430	108	900	0.0201	50
20	0.0425	106	1000	0.0183	46

Table ST5: Fluorescence quantum yield (ϕ_F) and Fluorescence Enhancement factor of **8** at 2.5×10^{-5} M concentration upon addition of Fe (II) and Cu (II) in dry THF.

Fe(II) added (μM)	ϕ_F	Fluorescence Enhancement	Cu (II) added (μM)	ϕ_F	Fluorescence Enhancement
0.0	0.00197	1	0.0	0.00197	1
5.0	0.01106	6	4	0.01572	8
9.0	0.01691	9	7	0.03486	18
12	0.02635	13	10	0.04601	23
15	0.04597	23	14	0.04967	25
18	0.12932	66	18	0.05706	29
24	0.20001	102	21	0.06163	31
26	0.25024	127	25	0.06759	34
30	0.26039	132	28	0.07453	38
40	0.26700	136	32	0.07845	40
50	0.26603	135	35	0.07938	40
60	0.26709	136	70	0.07915	40
70	0.26060	132	105	0.07926	40
80	0.26431	134	140	0.0802	40
100	0.26190	133	175	0.07966	40
200	0.25907	132			

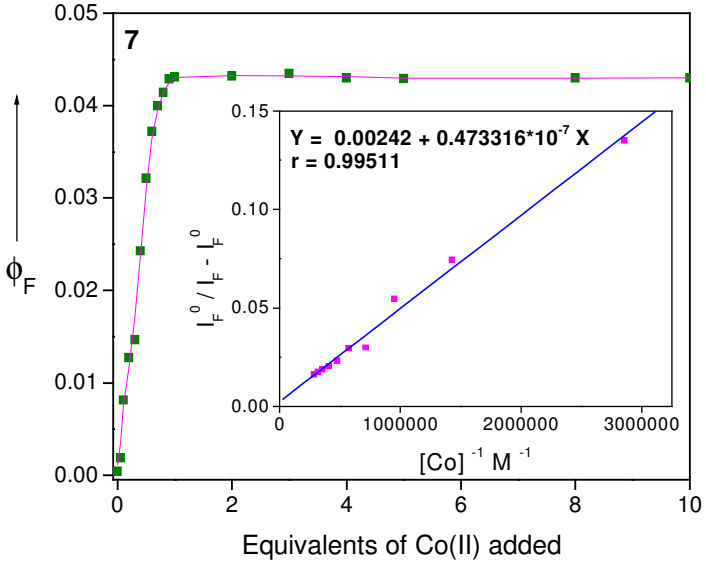

Figure S28: Plot of fluorescence quantum yield of **7** at 3.5×10^{-6} M concentration vs. amount of Co (II) added in dry THF. The nature of the curve indicates that **7** forms 1:1 complexation with Co (II). (Inset) Linear regression plot of $I_F^0 / (I_F - I_F^0)$ versus $[Co]^{-1}$ for **7.**

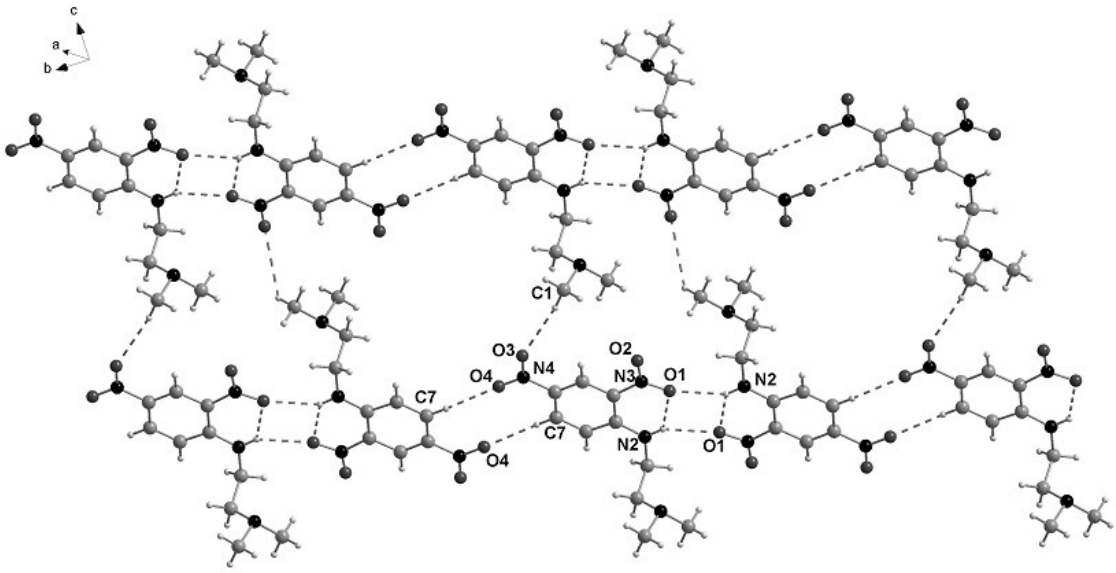

(a)

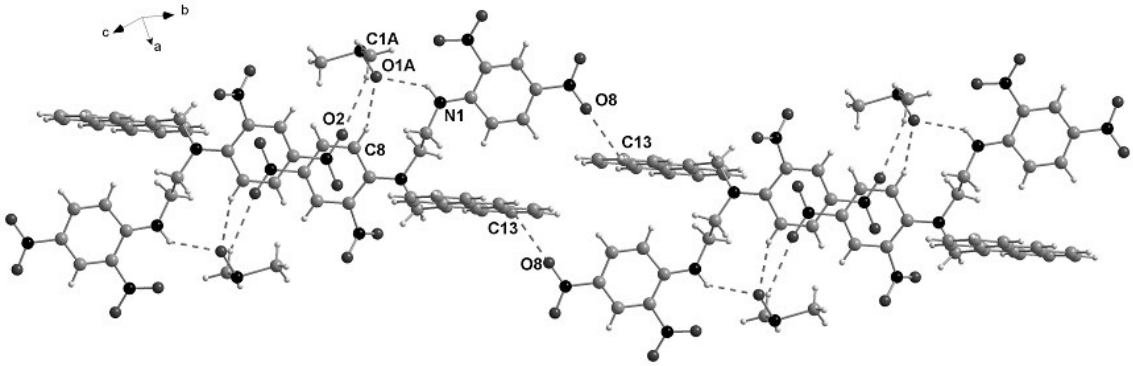

(b)

Figure S29: Perspective view of (a) 2D intra- and inter- molecular hydrogen bonded network of **5**, (b) solvent assisted hydrogen bonded 2D network of **8**.